Computation of Resonant Frequencies of Any Shaped Dielectric Resonators by CFDTD

A. Shahvarpour and M. S. Abrishamian
K. N. Toosi University of Technology, Iran

Abstract—Dielectric resonators (DR) have helped achieving the miniaturization of many active and passive microwave components, such as oscillators, filters and antennas. Nowadays they are used widely in mobile telecommunications and optical instruments such as optical couplers and filters. To design such components, designers must have the knowledge of predicting the shape and resonant frequency response of usable dielectric resonators. Numerical methods such as Method Of Moment (MOM), Finite Element Method (FEM) and Finite Difference Time Domain (FDTD), are useful tools for simulating those problems. The MOM & FEM are usually in frequency domain and we need to inverse a large matrix to solve the problem. Fortunately, FDTD is in time domain and by one run, we can have a large bandwidth response of our system. We have prepared a program code for determining resonant frequencies of DRs by using Conformal Finite Difference Time Domain (CFDTD) which is used for curved surfaces such as cylindrical and spherical shapes in Cartesian coordinate. In this paper, first, we present the simulation of resonant frequencies of cylindrical dielectric resonator which its results can be compared with reference results. In proceeding, computation of resonant frequency response of a thin dielectric spherical layer that can be useful for improving the achievement of Whispering Gallery Modes, which are produced in spherical DRs, will be considered.

1. Introduction

Dielectric resonators are used widely in mobile telecommunications and optical instruments, such as antennas, filters and couplers. Knowledge of predicting the shape and resonant frequency response of usable dielectric resonators is very important for engineers to design these telecommunication systems. Finite Difference Time Domain method is one of the numerical methods and even the most useful one for determining resonant frequencies of DRs, because by one run, we can have a large bandwidth response of our system.

In this work, we have prepared a code program for determining resonant frequencies of DRs by FDTD method, and for cases with curved surfaces such as cylindrical and spherical shapes we have used Conformal FDTD to reduce the error introduced by staircasing of surfaces that are not precisely aligned with major grid planes. To achieve such a goal, we have used the method suggested by Ref. [1] for simple structures. We have expanded that method for Yee cells which contain three or more layers of dissimilar dielectrics. We have used this method for simulation of thin layer dielectric curved surfaces, such as shelled spheres, that can be useful for improving the achievement of Whispering Gallery Modes.

The analytic method for computation of resonant frequencies of any spherical layers, which is used for verification of numerical method, is discussed in section 2. The CFDTD method applied for computation of resonant frequencies of any shaped DRs is in section 3 and finally in section 4, results of simulating are compared with analytic method and Ref. [4].

2. Analytical Computation of Resonant Frequencies of Multi Spherical Shells

In this section we only consider a dielectric sphere with a single coating layer. We use the Mie theory to compute the resonant frequencies. According to Ref. [2], we introduce two vectors **M** and **N** which correspond to TE and TM spherical modes.

$$\mathbf{M} = \mathbf{M}_e + j\mathbf{M}_o \tag{1}$$

$$\mathbf{N} = \mathbf{N}_e + \mathbf{j}\mathbf{N}_o \tag{2}$$

where

$$\mathbf{M}_{omn} = \frac{m\hat{a}_\theta}{\sin(\theta)}\mathrm{Z}_n(\beta r)\mathrm{P}_n^m(\cos(\theta))\cos(m\varphi) - \hat{a}_\varphi \mathrm{Z}_n(\beta r)\frac{\partial}{\partial_\theta}\mathrm{P}_n^m(\cos(\theta))\sin(m\varphi) \tag{3}$$

$$\mathbf{M}_{emn} = -\frac{m\hat{a}_\theta}{\sin(\theta)}\mathrm{Z}_n(\beta r)\mathrm{P}_n^m(\cos(\theta))\sin(m\varphi) - \hat{a}_\varphi \mathrm{Z}_n(\beta r)\frac{\partial}{\partial_\theta}\mathrm{P}_n^m(\cos(\theta))\cos(m\varphi) \tag{4}$$

$$\begin{aligned}
\mathbf{N}_{omn} &= \hat{a}_r \frac{n(n+1)}{\beta r} \mathrm{Z}_n(\beta r) \mathrm{P}_n^m(\cos(\theta)) \sin(m\varphi) + \hat{a}_\theta \frac{1}{\beta r} \frac{\partial}{\partial r} [r \mathrm{Z}_n(\beta r)] \frac{\partial}{\partial \theta} \mathrm{P}_n^m(\cos(\theta)) \sin(m\varphi) \\
&\quad + \hat{a}_\varphi \frac{m}{\sin(\theta)} \frac{1}{\beta r} [r \mathrm{Z}_n(\beta r)] \frac{\partial}{\partial \theta} \mathrm{P}_n^m(\cos(\theta)) \cos(m\varphi) \qquad (5) \\
\mathbf{N}_{emn} &= \hat{a}_r \frac{n(n+1)}{\beta r} \mathrm{Z}_n(\beta r) \mathrm{P}_n^m(\cos(\theta)) \cos(m\varphi) + \hat{a}_\theta \frac{1}{\beta r} \frac{\partial}{\partial r} [r \mathrm{Z}_n(\beta r)] \frac{\partial}{\partial \theta} \mathrm{P}_n^m(\cos(\theta)) \cos(m\varphi) \\
&\quad - \hat{a}_\varphi \frac{m}{\sin(\theta)} \frac{1}{\beta r} [r \mathrm{Z}_n(\beta r)] \frac{\partial}{\partial \theta} \mathrm{P}_n^m(\cos(\theta)) \sin(m\varphi) \qquad (6)
\end{aligned}$$

In these equations, Z_n indicates the spherical Bessel or Hankel functions correspond to the direction of propagating wave. Also P_n^m is Associate Legendre function. In proceeding we use substitution indicated by Eq. (7):

$$\hat{\mathrm{Z}}_n(\beta r) = \beta r \mathrm{Z}_n(\beta r) \qquad (7)$$

According to Fig. 1 we can expand electromagnetic fields by two vectors **M** and **N**:

$$\begin{aligned}
\mathbf{E}^i &= \sum_{n=1}^{\infty} \alpha_n \left[\mathbf{M}_{\mathrm{o}1n}^{(1)}(\beta_3, \mathbf{r}, \theta, \varphi) + j \mathbf{N}_{\mathrm{e}1n}^{(1)}(\beta_3, \mathbf{r}, \theta, \varphi) \right] \qquad (8) \\
\mathbf{H}^i &= \frac{j}{\eta_3} \sum_{n=1}^{\infty} \alpha_n \left[\mathbf{N}_{\mathrm{o}1n}^{(1)}(\beta_3, \mathbf{r}, \theta, \varphi) + j \mathbf{M}_{\mathrm{e}1n}^{(1)}(\beta_3, \mathbf{r}, \theta, \varphi) \right] \qquad (9)
\end{aligned}$$

$\mathbf{E}^i$ and $\mathbf{H}^i$ are incident plane wave electromagnetic fields. Also in these equations β is wave number, η is characteristic impedance and coefficient α_n defined as:

$$\alpha_n = (-j)^n \frac{2n+1}{n(n+1)} \qquad (10)$$

Scattered and transmitted waves in each layer can be expanded as Eqs. (11) to (18):

$$\begin{aligned}
\mathbf{E}^{s_3} &= \sum_{n=1}^{\infty} \left[A_n^{s_3} \mathbf{M}_{\mathrm{o}1n}^{(4)}(\beta_3, \mathbf{r}, \theta, \varphi) + j B_n^{s_3} \mathbf{N}_{\mathrm{e}1n}^{(4)}(\beta_3, \mathbf{r}, \theta, \varphi) \right] \qquad (11) \\
\mathbf{H}^{s_3} &= \frac{j}{\eta_3} \sum_{n=1}^{\infty} \left[A_n^{s_3} \mathbf{N}_{\mathrm{o}1n}^{(4)}(\beta_3, \mathbf{r}, \theta, \varphi) + j B_n^{s_3} \mathbf{M}_{\mathrm{e}1n}^{(4)}(\beta_3, \mathbf{r}, \theta, \varphi) \right] \qquad (12) \\
\mathbf{E}^{t_2} &= \sum_{n=1}^{\infty} \left[A_n^{t_2} \mathbf{M}_{\mathrm{o}1n}^{(1)}(\beta_2, \mathbf{r}, \theta, \varphi) + j B_n^{t_2} \mathbf{N}_{\mathrm{e}1n}^{(1)}(\beta_2, \mathbf{r}, \theta, \varphi) \right] \qquad (13) \\
\mathbf{H}^{t_2} &= \frac{j}{\eta_2} \sum_{n=1}^{\infty} \left[A_n^{t_2} \mathbf{N}_{\mathrm{o}1n}^{(1)}(\beta_2, \mathbf{r}, \theta, \varphi) + j B_n^{t_2} \mathbf{M}_{\mathrm{e}1n}^{(1)}(\beta_2, \mathbf{r}, \theta, \varphi) \right] \qquad (14) \\
\mathbf{E}^{s_2} &= \sum_{n=1}^{\infty} \left[A_n^{s_2} \mathbf{M}_{\mathrm{o}1n}^{(4)}(\beta_2, \mathbf{r}, \theta, \varphi) + j B_n^{s_2} \mathbf{N}_{\mathrm{e}1n}^{(4)}(\beta_2, \mathbf{r}, \theta, \varphi) \right] \qquad (15) \\
\mathbf{H}^{s_2} &= \frac{j}{\eta_2} \sum_{n=1}^{\infty} \left[A_n^{s_2} \mathbf{N}_{\mathrm{o}1n}^{(4)}(\beta_2, \mathbf{r}, \theta, \varphi) + j B_n^{s_2} \mathbf{M}_{\mathrm{e}1n}^{(4)}(\beta_2, \mathbf{r}, \theta, \varphi) \right] \qquad (16) \\
\mathbf{E}^{t_1} &= \sum_{n=1}^{\infty} \left[A_n^{t_1} \mathbf{M}_{\mathrm{o}1n}^{(1)}(\beta_1, \mathbf{r}, \theta, \varphi) + j B_n^{t_1} \mathbf{N}_{\mathrm{e}1n}^{(1)}(\beta_1, \mathbf{r}, \theta, \varphi) \right] \qquad (17) \\
\mathbf{H}^{t_1} &= \frac{j}{\eta_1} \sum_{n=1}^{\infty} \left[A_n^{t_1} \mathbf{N}_{\mathrm{o}1n}^{(1)}(\beta_1, \mathbf{r}, \theta, \varphi) + j B_n^{t_1} \mathbf{M}_{\mathrm{e}1n}^{(1)}(\beta_1, \mathbf{r}, \theta, \varphi) \right] \qquad (18)
\end{aligned}$$

where, in Eqs. (11) to (18), superscript (1) stands for spherical Bessel functions j_n and superscript (4) for spherical Hankel functions $h_n^{(2)}$, which we faced in **M** and **N** [2]. And also s and t superscripts in coefficients stand for scattered and transmitted waves in each layer.

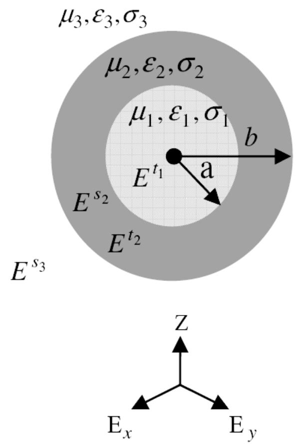

Figure 1: A plane wave incident to the two layer spherical dielectric resonator.

Let us assume that $\mu_1 = \mu_2 = \mu_3 = \mu_0$ and $\sigma_1 = \sigma_2 = \sigma_3 = 0$, by applying the boundary conditions we will have two different matrixes for TE and TM modes, separately.

$$\begin{bmatrix} -h_n^{(2)}(\beta_3 b) & h_n^{(2)}(\beta_2 b) & j_n(\beta_2 b) & 0 \\ -\hat{h}'^{(2)}_n(\beta_3 b) & \hat{h}'^{(2)}_n(\beta_2 b) & \hat{j}'_n(\beta_2 b) & 0 \\ 0 & h_n^{(2)}(\beta_2 a) & j_n(\beta_2 a) & -j_n(\beta_1 a) \\ 0 & \hat{h}'^{(2)}_n(\beta_2 a) & \hat{j}'_n(\beta_2 a) & -\hat{j}'_n(\beta_1 a) \end{bmatrix} \begin{bmatrix} A_n^{s_3} \\ A_n^{s_2} \\ A_n^{t_2} \\ A_n^{t_1} \end{bmatrix} = \begin{bmatrix} \alpha_n j_n(\beta_3 b) \\ \alpha_n \hat{j}'_n(\beta_3 b) \\ 0 \\ 0 \end{bmatrix} \tag{19}$$

$$\begin{bmatrix} -\hat{h}'^{(2)}_n(\beta_3 b) & \sqrt{\frac{\varepsilon_3}{\varepsilon_2}}\hat{h}'^{(2)}_n(\beta_2 b) & \sqrt{\frac{\varepsilon_3}{\varepsilon_2}}\hat{j}'_n(\beta_2 b) & 0 \\ -h_n^{(2)}(\beta_3 b) & \sqrt{\frac{\varepsilon_2}{\varepsilon_3}}h_n^{(2)}(\beta_2 b) & \sqrt{\frac{\varepsilon_2}{\varepsilon_3}}j_n(\beta_2 b) & 0 \\ 0 & \sqrt{\frac{\varepsilon_1}{\varepsilon_2}}\hat{h}'^{(2)}_n(\beta_2 a) & \sqrt{\frac{\varepsilon_1}{\varepsilon_2}}\hat{j}'_n(\beta_2 a) & -\hat{j}'_n(\beta_1 a) \\ 0 & \sqrt{\frac{\varepsilon_2}{\varepsilon_1}}h_n^{(2)}(\beta_2 a) & \sqrt{\frac{\varepsilon_2}{\varepsilon_1}}j_n(\beta_2 a) & -j_n(\beta_1 a) \end{bmatrix} \begin{bmatrix} B_n^{s_3} \\ B_n^{s_2} \\ B_n^{t_2} \\ B_n^{t_1} \end{bmatrix} = \begin{bmatrix} \alpha_n \hat{j}'_n(\beta_3 b) \\ \alpha_n j_n(\beta_3 b) \\ 0 \\ 0 \end{bmatrix} \tag{20}$$

The solution of these two complex equations will give us the resonant frequencies and quality factors of multilayer dielectric resonators.

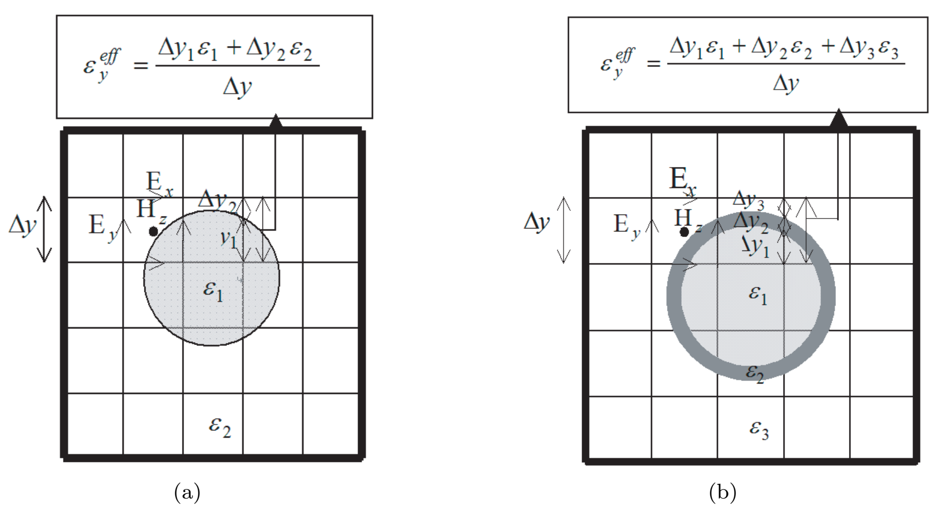

Figure 2: (a) Mesh truncation of a spherical DR and (b) Mesh truncation of a thin layer spherical DR.

3. CFDTD Method

The CFDTD can reduce the error introduced by staircasing in Cartesian coordinate. The effective dielectric permittivity of dielectric material in any piece of stairs can be found by following equations [1].

$$\varepsilon_x^{eff} = \frac{\Delta x_1 \varepsilon_1 + \Delta x_2 \varepsilon_2}{\Delta x} \tag{21}$$

$$\varepsilon_y^{eff} = \frac{\Delta y_1 \varepsilon_1 + \Delta y_2 \varepsilon_2}{\Delta y} \tag{22}$$

$$\varepsilon_z^{eff} = \frac{\Delta z_1 \varepsilon_1 + \Delta z_2 \varepsilon_2}{\Delta z} \tag{23}$$

where, by applying these values in split Maxwell equations, the error of staircasing will be reduced.

In the case of thin layer surface, such as a spherical shell DR, Yee cells may contain three or more dissimilar dielectrics. In such cases, such as n different dielectric layers, we use average method.

$$\varepsilon_x^{eff} = \frac{\Delta x_1 \varepsilon_1 + \Delta x_2 \varepsilon_2 + \Delta x_3 \varepsilon_3 + \ldots + \Delta x_n \varepsilon_n}{\Delta x} \tag{24}$$

$$\varepsilon_y^{eff} = \frac{\Delta y_1 \varepsilon_1 + \Delta y_2 \varepsilon_2 + \Delta y_3 \varepsilon_3 + \ldots + \Delta y_n \varepsilon_n}{\Delta y} \tag{25}$$

$$\varepsilon_z^{eff} = \frac{\Delta z_1 \varepsilon_1 + \Delta z_2 \varepsilon_2 + \Delta z_3 \varepsilon_3 + \ldots + \Delta z_n \varepsilon_n}{\Delta z} \tag{26}$$

Table 1: Comparison of resonant frequencies found by CFDTD simulation and Ref. [4], for a cylindrical DR with $\varepsilon_r = 38$, $a = 5.25$ mm and $h = 4.6$ mm.

Mode	Frequency (GHz)		Relative Error
	Ref. [4]	CFDTD	
$TE_{01\delta}$	4.829	4.859	%0.621
$HEM_{11\delta}$	6.333	6.299	%0.536
$HEM_{12\delta}$	6.638	6.694	%0.843
$TM_{01\delta}$	7.524	7.487	%0.491
$HEM_{21\delta}$	7.752	7.702	%0.644

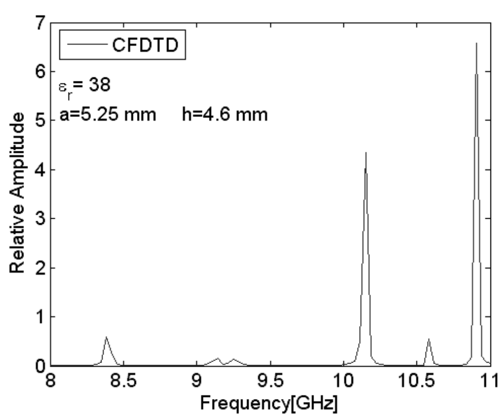

(a)

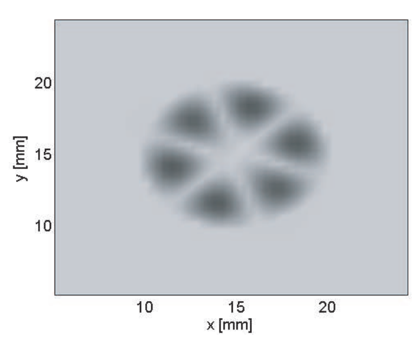

(b)

Figure 3: (a) Resonant frequency response of a cylindrical DR with $\varepsilon_r = 38$, $a = 5.25$ mm and $h = 4.6$ mm found by CFDTD and (b) Plot of H field at $f = 10.1507$ GHz.

4. Numerical Results

In this section the results of CFDTD simulation for cylindrical and thin layer spherical DRs are shown. For verification, the results are compared with analytical (exact) method or with other reference data.

4.1. Cylindrical Dielectric Resonator

Let us use cylindrical DR with following electrical and geometrical parameters: $\varepsilon_r = 38$, radius $a = 5.25\,\mathrm{mm}$ and height $h = 4.6\,\mathrm{mm}$. In table 1, resonant frequencies found by CFDTD simulation and Ref. [4] are compared. Also in Fig. 3, frequency response of the cylindrical DR and plot of H field, stimulated at f=10.1507 GHz, are shown.

4.2. Thin Layer Spherical Dielectric Resonator

A thin layer spherical DR with $\varepsilon_r = 90$, external radius $b = 2.54\,\mathrm{cm}$ and internal radius $a = 0.99b$ is simulated with CFDTD method. We have compared our results with Mie method and it is fairly good. As it is shown in Fig. 4(b), Whispering Gallery Mode is stimulated in the thin layer spherical DR at $f = 35.3214\,\mathrm{GHz}$.

5. Conclusion

In this article, we have presented CFDTD simulation of dielectric resonators. A cylindrical DR has been simulated, and a good agreement with Ref. [4] is achieved. For the next simulation, a thin layer spherical dielectric resonator is considered and we faced with Whispering Gallery Modes which we have predicted by Mie method.

These simulations will show us that CFDTD method can give us very good results for simulating resonant frequencies of any shaped dielectric resonators.

Acknowledgment

The authors wish to thank Iran Telecommunications Research Center for encouragement and sponsoring this work.

REFERENCES

1. Dey, S. and R. Mittra, "A conformal finite difference time domain technique for modeling cylindrical dielectric resonators," *IEEE Transactions on Microwave Theory & Techniques*, Vol. 47, No. 9, 1737–1739, September 1999.
2. Stratton, J. A., *Electromagnetic Theory*, McGraw-Hill, New York, 1941.
3. Tobar, M. E., J. D. Hartnett, and J. Anstie, "Proposal for a michelson-morley experiment using whispering spherical mode resonators," *Physics Letters A*, Vol. 300/1, 33–39, 2000.
4. Kajfez, D. and P. Guillon, *Dielectric Resonators*, Artech House, Norwood, MA, 1986.
5. Taflove, A. and S. C. Hagness, *Computation Electrodynamics: The Finite-Difference Time-Domain Method*, Artech House, Norwood, MA, 2000.
6. Berenger, J. P., "Perfectly matched layer for absorption of electromagnetic waves," *Journal of Computational Physics*, Vol. 114, No. 2, 185–200, 1994.